Comprehensive chemical characterization of industrial $PM_{2.5}$ from steel industry activities

Alexandre Sylvestre [a, d, *], Aurélie Mizzi [a], Sébastien Mathiot [b], Fanny Masson [c], Jean L. Jaffrezo [c], Julien Dron [d], Boualem Mesbah [b], Henri Wortham [a], Nicolas Marchand [a, **]

[a] Aix Marseille Univ, CNRS, LCE, Marseille, France
[b] AirPACA, Air Quality Observatory in Provence Alpes Côte d'Azur, Marseille, France
[c] Univ. Grenoble Alpes, CNRS, LGGE, UMR 5183, F-38000 Grenoble, France
[d] Institut Ecocitoyen pour la Connaissance des Pollutions, 13270 Fos-sur-Mer, France

HIGHLIGHTS

- Exhaustive $PM_{2.5}$ chemical profiles emitted by steelworks subunits are investigated.
- Sulfate is emitted by the oxygen converter process but also by combustion processes.
- PAHs and sulfur containing PAH are emitted by combustion processes.
- Calcium is emitted by all subunits but differences are obtained for Ca/Ca^{2+} ratios.
- Al, Fe, Zn, Mn, Ti are emitted by all subunits, proportion dependent of processes.

GRAPHICAL ABSTRACT
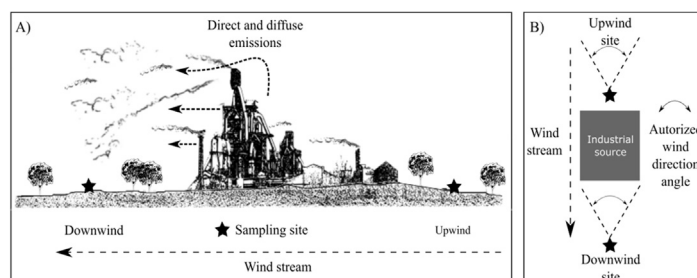
ARTICLE INFO

ABSTRACT

Industrial sources are among the least documented PM (Particulate Matter) source in terms of chemical composition, which limits our understanding of their effective impact on ambient PM concentrations. We report 4 chemical emission profiles of $PM_{2.5}$ for multiple activities located in a vast metallurgical complex. Emissions profiles were calculated as the difference of species concentrations between an upwind and a downwind site normalized by the absolute $PM_{2.5}$ enrichment between both sites. We characterized the $PM_{2.5}$ emissions profiles of the industrial activities related to the cast iron (complex 1) and the iron ore conversion processes (complex 2), as well as 2 storage areas: a blast furnace slag area (complex 3) and an ore terminal (complex 4). $PM_{2.5}$ major fractions (Organic Carbon (OC) and Elemental Carbon (EC), major ions), organic markers as well as metals/trace elements are reported for the 4 industrial complexes. Among the trace elements, iron is the most emitted for the complex 1 (146.0 mg g^{-1} of $PM_{2.5}$), the complex 2 (70.07 mg g^{-1}) and the complex 3 (124.4 mg g^{-1}) followed by Al, Mn and Zn. A strong emission of Polycyclic Aromatic Hydrocarbons (PAH), representing 1.3% of the Organic Matter (OM), is observed for the iron ore transformation complex (complex 2) which merges the activities of coke and iron sinter production and the blast furnace processes. In addition to unsubstituted PAHs, sulfur containing PAHs (SPAHs) are also significantly emitted (between 0.011 and 0.068 mg g^{-1}) by the complex

---

2 and could become very useful organic markers of steel industry activities. For the complexes 1 and 2 (cast iron and iron ore converters), a strong fraction of sulfate ranging from 0.284 to 0.336 g g^{-1}) and only partially neutralized by ammonium, is observed indicating that sulfates, if not directly emitted by the industrial activity, are formed very quickly in the plume. Emission from complex 4 (Ore terminal) are characterized by high contribution of Al (125.7 mg g^{-1} of PM$_{2.5}$) but also, in a lesser extent, of Fe, Mn, Ti and Zn. We also highlighted high contribution of calcium ranging from 0.123 to 0.558 g g^{-1} for all of the industrial complexes under study. Since calcium is also widely used as a proxy of the dust contributions in source apportionment studies, our results suggest that this assumption should be reexamined in environments impacted by industrial emissions.

1. Introduction

Improvement of air quality is an important concern in many environments. In order to limit the impact of air quality on human health, public authorities need reliable and accurate information regarding the PM (particulate Matter) sources contributions. In the last two decades, the development of source apportionment approaches (Canonaco et al., 2013; Paatero and Tapper, 1994; Schauer et al., 1996) has considerably improved our knowledge of the relative impact of the various primary PM sources. One constant of the main sources apportionment approaches developed (Chemical Mass Balance, Positive Matrix Factorization or Multilinear Engine) is the *a priori* knowledge, at different extent of accuracy, of the chemical profiles of each emissions sources. However, comparisons between these different source apportionment approaches showed significant differences especially in regards to the industrial sources. For example, a comparative study between CMB and PMF approaches (Okamoto et al., 2012) showed that even if the sources contributions are well correlated, PMF attributed to the steel mill source about 2.5 times more PM mass than in results derived from a CMB analysis. This gap is explained by differences in the steel mill aerosol chemical profiles which mainly differ by the distribution of specific trace elements (ie. Ti and Fe, mostly). Similar discrepancies were observed by another inter-comparison study of source apportionment approaches (PMF, CMB and PCA) in an industrial area (Viana et al., 2008).

Numerous studies have been carried out to characterize the chemical source profiles of vehicular emissions (El Haddad et al., 2009; Liu et al., 2010; Lough et al., 2007; Rogge et al., 1993a, 1993b; Schauer et al., 1999b, 2002b), biomass burning (Robinson et al., 2006a; Rogge et al., 1998; Schauer et al., 2001; Simoneit et al., 1999; Nolte et al., 2001) and food cooking (Nolte et al., 1999; Robinson et al., 2006b; Rogge et al., 1991; Schauer et al., 1999a, 2002a). Among the main primary aerosol anthropogenic sources, industrial emissions are the least documented in the literature. This lack is mainly due to the difficulty to get representative source profiles. The number of industrial sources associated with a wide range of processes which are, in most cases, not continuous accentuate this difficulty. For example, in metallurgy, two distinct processes exist to produce molten steel: the basic oxygen furnace and the electric arc furnace. Previous studies (Larsen et al., 2008; Yatkin and Bayram, 2008) have shown that, if both processes emit the same trace elements such as calcium (Ca), iron (Fe) and zinc (Zn), their proportions are significantly different according to the processes considered. The basic oxygen furnace emits more calcium while the electric arc furnace emits more iron and zinc. The Ca/Fe ratio is indeed 73 times higher for the basic oxygen furnace. Emission of lead (Pb) is also observed in high proportion for the electric arc furnace (0.08 g g^{-1}; Yatkin and Bayram, 2008) but is only weakly emitted by the basic oxygen furnace (0.001 g g^{-1}; Larsen et al., 2008). Insights in aerosol

chemical composition of industrial activities have been provided using either field measurements conducted in the vicinity of an industrial complex or either measurements carried out directly in the stack (Riffault et al., 2015; Hleis et al., 2013; Baraniecka et al., 2010; Dall'Osto et al., 2008; Okamoto et al., 2012; Rogge et al., 1997a, 1997b; Sánchez de la Campa et al., 2010; Weitkamp et al., 2005; Yang et al., 2002, 1998; Yoo et al., 2002; Leoni et al., 2016). Some studies highlighted the importance of trace elements and metals such as Al, Fe, Ca, Ni, V, Zn, Pb or Mg (Dall'Osto et al., 2008; Guinot et al., 2016; Hleis et al., 2013; Kfoury et al., 2016; Mbengue et al., 2017; Pokorná et al., 2015; Taiwo et al., 2014; Weitkamp et al., 2005; Yoo et al., 2002) while others revealed high emission rates of organic compounds such as Polycyclic Aromatic Hydrocarbons (PAHs) (Baraniecka et al., 2010; Leoni et al., 2016; Yang et al., 1998, 2002). The characterization of both inorganic and organic aerosol fractions is thus required in order to build comprehensive and representative industrial source profiles.

Industrial emissions profiles have mostly been established by mean of direct measurements in the stacks (Buonanno et al., 2011; Chen et al., 2013; Tsai et al., 2007; Yang et al., 1998, 2002). While this approach provides straightforward and detailed information of the composition of the emissions associated to one specific industrial process, it suffers from 2 biases that limit the use of the chemical profile obtained. Due to the high concentrations and temperatures prevailing in industrial stacks, emissions do not reach a thermodynamic equilibrium, thus the gas-particle partitioning cannot be considered as representative of the ambient atmosphere. This results mainly in an overestimation of the Organic Carbon (OC) and other semi volatile organic compounds emission factors. Furthermore, the global impact of an industrial complex cannot be assessed by only considering the emissions of the main stack exhausts. Diffuse and fugitive emissions can be captured by the study of the enrichments of atmospheric pollutants downwind from an industrial complex, using an upwind reference. This kind of methodology has been successfully adopted in several studies such as Weitkamp et al. (2005), Alleman et al. (2010), Dall'Osto et al. (2008) or Lim et al. (2010). Such enrichment based approaches are more difficult to implement and the choice of both up and downwind sites must be addressed with cautions. While the upwind measurements site must be representative of the regional background air pollution, the downwind site must be located close to the studied sources in order to avoid interferences from other sources but far enough to capture the diversity of the industrial emissions (direct, diffuse and fugitive).

Here we report 4 chemical profiles of PM emitted by 4 subunits of a vast metallurgical complex obtained by mean of an enrichment based approach. A particular emphasis has been put in the chemical characterization of aerosol which combines, in addition to the major fractions, a large array of trace elements, metals and organic markers.

2. Materials and methods

2.1. Metallurgic complex

The metallurgic complex, located in the South or France (43°25′57.1″N 4°53′04.8″E) is presented in Fig. 1. Its surface area is 11 km2 and its production capacity is up to 4 million tons per year

of steel. Four subunits of this vast complex were individually studied (Fig. 1 and Table 1): the first one encompasses all the in-ladle metallurgic treatment installation and the oxygen converters (complex 1, *Cast iron converter complex*), the second one regroups the discharging quay, the coke plant, the sinter plant and the blast furnaces (complex 2, *iron ore converter complex*), the third one is the blast furnace slag storage area (complex 3, *blast*
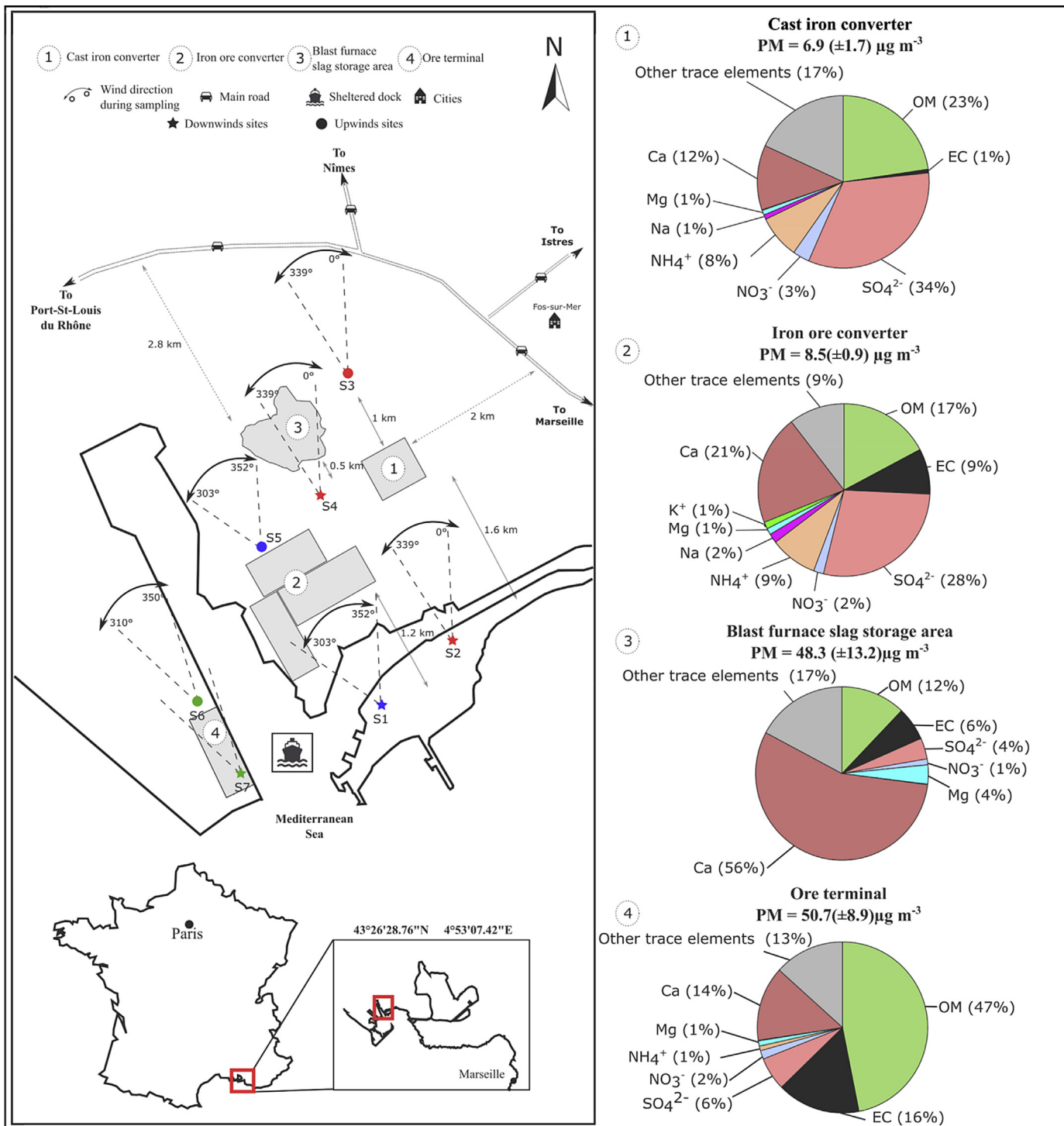

Fig. 1. (2-column fitting image): Location of each industrial complex and sampling site. S2, S1, S4 and S7 are the downwind sampling sites for the complex 1, 2, 3 and 4, respectively. S3, S5 and S6 are the upwind sampling sites for the complex 1/3, 2 and 4, respectively. For each source and mobile unit, the wind directions sector authorized for sampling is also represented. Pie charts represent the contribution of main aerosol fraction to the total PM$_{2.5}$ mass emitted by each source 1) Cast iron converter complex (complex 1), 2) Iron ore converter complex (complex 2), 3) Blast furnace slag storage area (complex 3) and 4) ore terminal (complex 4).

Table 1
Codes, sources and processes involved, type of emissions and mains materials used for each complex.

Code	Sources and processes involved	Type of emissions	Mains materials used
Cast iron converter complex	In-ladle metallurgic treatment installation	Direct and fugitive	Cast iron
	Oxygen converters	Direct and fugitive	Cast iron
Iron ore converter complex	Discharging quay	fugitive	Iron ore, limestone
	Coke plant	Direct and fugitive	Coal
	Sinter plant	Direct and fugitive	Iron ore
	Blast furnaces	Direct and fugitive	Iron ore, coke
Blast furnace slag storage area	blast furnace slag storage area	fugitive	wastes from blast furnace
Ore terminal	Ore terminal	fugitive	lime, petroleum coal, coke and bauxite

furnace slag storage area) and the last one is an ore terminal (complex 4, **Ore Terminal**). This ore terminal has a surface area of 0.8 km^2. The main ores stored are lime, petroleum coal, coke and bauxite. More information regarding the operation procedures of the various complexes are provided in the supporting information.

2.2. Sampling strategy

Two instrumented mobile units were deployed for the characterization of the emissions of each complex. A first mobile unit was installed upwind of the complex to collect the aerosol regional background concentrations while the second mobile unit was installed downwind of the complex in order to sample the aerosol regional background enriched with the industrial complex emissions (Fig. 1). Both upwind and downwind sampling site locations were selected according to the prevailing wind directions observed during the same season over the past 30 years. Downwind sampling sites were chosen to avoid or minimize any potential influence of others sources. Distances between the sampling sites and the sources under study were always less than 2 km (Fig. 1). Further information regarding each sampling site are reported in the supporting information (Table A.1). The experimental setup was deployed during a total of 9 consecutive months in the area, (from May 2013 to January 2014), in order to collect enough representative samples.

Each mobile unit was equipped with a PM$_{2.5}$ high volume sampler (DA-80 DIGITEL, 30 m^3 h^{-1}). Each high volume sampler was triggered by a wind vane so that the effective sampling occurred under very specific and controlled wind conditions (Fig. 1 and Table A.1). The authorized wind directions angles may vary from one complex to another according to the specificity of the source and the relative positions of the mobile units, but was always within a sector of less than 50°. These sectors were identical for both up and downwind sites. A wind speed threshold of 2 m s^{-1} was also set. Samples (150 mm Pallflex® Tissuquartz™ pre-baked at 500 °C during 5 h) were automatically changed after 4 h of effective sampling (ie. 120 m^3). After collection, the samples were wrapped in an aluminum foil, sealed in polyethylene bags and stored at −18 °C until analysis. Field blanks collected during the campaign were stored following the same procedure.

The mobile units located downwind were further equipped with an Ultrafine Particle Monitor (UFP, TSI, Model 3031) allowing the study of the aerosol size distribution separated within 6 size bins (20−30 nm, 30−50 nm, 50−70 nm, 70−100 nm, 100−200 nm and 200−1000 nm), together with SO$_2$ and NOx analyzers (Environment SA).

A total of 28 couples of samples (up and downwind) were collected. They are distributed as follows: 7, 8, 4, 9 couples for the complexes 1, 2, 3 and 4, respectively. Samples selection was done with the following criteria in mind:

1/ Synchronization of the samples collection period at both sites. Although both HV-Samplers were triggered by a wind vane, few pair of samples were not perfectly synchronized. A tolerance of 1 h between the sampling periods at both sites has been set. Beyond 1 h, we have considered that the regional background subtraction was not legitimate anymore.

2/ Sampling time. The time period necessary to sample the required 120 m^3 must be less than 6 h in order to sample homogeneous air masses. It should be noted that in the case of sampling time periods longer than 6 h, the first criteria was not respected.

3/ Evidence of specific events impacting the downwind site. The last step of the selection procedure is based on the observation of sharp increases of either particles number concentrations, SO2 concentrations, or NOx concentrations at the downwind site. As discussed above only the downwind site were equipped by online analyzers. The occurrence of such sharp events do not guarantee the collection of PM impacted by the emissions of the industrial complex, but the lack of such events at the downwind site implies the absence of a significant impact of those emissions.

2.3. Sample analysis

Organic carbon (OC) and elemental carbon (EC) were measured using the Thermo-Optical Transmission (TOT) method with a Sunset Lab analyzer (Aymoz et al., 2007) following the EUSAAR2 temperature program (Cavalli et al., 2010). Ion chromatography (IC) was used to analyze the major ions (SO$_4^{2-}$, NO$_3^-$, NH$_4^+$, Na$^+$, K$^+$, Mg^{2+} and Ca^{2+}) following the method described in a previous work (Jaffrezo et al., 1998). Trace elements (Ca, Mg, K, Al, As, Ba, Cd, Ce, Co, Cr, Cs, Cu, Fe, La, Li, Mn, Mo, Ni, Pb, Rb, Sb, Sc, Se, Sn, Sr, Ti, Tl, V, Zn, Zr) were analyzed by ICP-MS as described in Waked et al. (2014). The complete methodology for EC, OC, major ions and trace elements analysis is also described in Waked et al. (2014). Organic compounds were quantified by gas chromatography coupled with mass spectrometry (GC-MS), following the method detailed in El Haddad et al. (2009, 2013). This method allows the quantification of PAHs, sulfur PAHs (SPAHs), hopanes and steranes, n-alkanes (C18-C36) as well as fatty acids, anhydride sugars, sterols, and syringyl and guaiacyl derivatives. The same analyses were performed with field blank samples (4 field blanks for the complexes 1,2 and 3 and 2 field blanks for the complex 4).

2.4. Determination of emission profiles

The contribution of a species i to the PM$_{2.5}$ emitted by a given source is calculated following equation. (1):

$$a_i = \frac{C_{i,d} - C_{i,u}}{PM_{2.5}} \tag{1}$$

Where, a_i (g g^{-1} or mg g^{-1}) is the contribution of the specie i to the PM$_{2.5}$ mass concentration emitted by the industrial complex, $C_{i,d}$ and $C_{i,u}$ are the concentrations (µg.m^{-3} or ng.m^{-3}) of the species i measured downwind *(d)* and upwind *(u)* of the industrial complex and PM$_{2.5}$ is the total PM$_{2.5}$ enrichment (µg.m^{-3}). The

PM$_{2.5}$ enrichment, for one couple of samples, is reconstituted by summing up the enrichments of the major fractions (ie. Organic Matter (OM), EC, sulfate, nitrate, ammonium and trace elements). An OM-to-OC conversion ratio of 1.2 was used here (Aiken et al., 2008). Only species presenting a significant relative enrichment between the two sampling sites ($\frac{C_{i,d}-C_{i,u}}{C_{i,u}} > 0.4$; i.e. relative difference at least equal to twice the maximum analytical error −20%-) were considered. Otherwise, the concentrations obtained for both downwind and the upwind sites were considered as not significantly different. In such cases, the compound is quoted < LQ in Tables 2,3 and 4. Contribution reported in Tables 2, 3 and 4 correspond to the average of the contribution calculated for each pair of samples.

3. Results and discussion

3.1. Particle mass enrichment and particle size distributions

Total PM$_{2.5}$ enrichments are significantly different from one group of sources to another. The cast iron converter complex (complex 1) shows a PM$_{2.5}$ absolute enrichment of 6.91 ± 1.67 μg m^{-3} and this enrichment is rather similar with the one observed for the iron ore converter (complex 2) which is 8.50 ± 0.90 μg m^{-3} (Table 2). For the two others source, mainly composed of storage areas (slag or ore), PM$_{2.5}$ enrichments are much higher, reaching 50 μg m^{-3}, with 48.35 ± 13.22 for the slag storage area (complex 3) and 50.70 ± 8.85 μg m^{-3} for the ore terminal (complex 4). Such high enrichments are most probaby due to the resuspension of coarse particles from the stored materials.

While the total submicron particles number concentrations observed downstream of the two storage areas are low (<6200 cm^{-3}), we observe a high concentration of submicron particle number concentration downwind of complex 1 and 2 with average concentrations of 19 200 and 32 000 cm^{-3}, respectively. Both distributions are clearly dominated by the ultrafine mode (<100 nm), which represents 94% of the total submicron particle number concentrations for the complex 1, and 96% for the complex 2, underlying the influence of freshly formed particles in the emissions of these two complexes (Fig. 2 A). We note that the number of ultrafine particles for complex 2 is twice as high as that of complex 1 (Fig. 2A). This difference is consistent with the one

observed for SO$_2$ concentrations (Fig. 2B). Such ultrafine particles events have already been observed in Marseille, the nearest major city, located 40 km away, when impacted by industrial emissions (El Haddad et al., 2011, 2013).

3.2. Major fractions

The aerosol composition is also significantly different from one group of sources to another (Table 2). Emissions from complex 1 and 2 are characterized by high proportion of sulfates, representing 0.336 ± 0.065 g g^{-1} and 0.284 ± 0.163 g g^{-1} of PM$_{2.5}$, respectively. Again these results are in line with the SO$_2$ concentrations measured downstream of the sources which are much higher for complex 1 and 2 (14 and 47 μg m^{-3}, respectively) than for complex 3 and 4 (<1 μg m^{-3}) (Fig. 2B). Note that sulfates are in both cases only partially neutralized by ammonium, which represents only 0.082 ± 0.036 g g^{-1} and 0.090 ± 0.064 g g^{-1} of the PM$_{2.5}$, respectively. The second most abundant fraction emitted by these two complexes is the carbonaceous fraction (OM and EC) which represents 0.236 g g^{-1} and 0.260 g g^{-1} of PM$_{2.5}$. However while the carbonaceous fraction is almost exclusively dominated by OM in the emissions of the cast iron converter complex (complex 1), a significant fraction of EC (0.086 ± 0.061) is observed for the iron ore converter (complex 2).

Very different aerosol compositions are observed when comparing the slag storage area (complex 3) and the ore terminal (complex 4) emissions (Table 2). Sulfates represent for these two complexes only a minor fraction with 0.039 ± 0.005 g g^{-1} and 0.063 ± 0.001 g g^{-1}, respectively. More surprisingly, we observe a strong contribution of OM and EC for the ore terminal (complex 4), which represent 0.469 ± 0.082 g g^{-1} and 0.158 ± 0.028 g g^{-1} respectively. Such contributions are probably related to the influence of the petroleum coke and coal stored in this area, as further suggested by the abundance of PAHs and SPAHs (see section 3.3). These carbonaceous materials represent only a minor fraction of the complex 3 emissions (0.121 ± 0.015 g g^{-1} for OM and 0.063 ± 0.008 g g^{-1} for EC), which is clearly dominated by calcium representing 56% of the PM$_{2.5}$ enrichment, sustaining the influence of resuspension processes in the slag storage area. Overall, calcium constitutes a significant fraction of the PM$_{2.5}$ emitted by all the sources investigated here. It represents 0.123 ± 0.021 g g^{-1},

Table 2
Mass balance of PM$_{2.5}$ (average (standard deviation)).

	Complex 1 Cast iron converter complex	Complex 2 Ore iron converter complex	Complex 3 Blast furnace slag storage area	Complex 4 Ore terminal
Reconstituted particle matter mass [μg m^{-3}]				
PM$_{2.5}$[a]	6.91 (±1.67)	8.50 (±0.90)	48.35 (±13.22)	50.70 (±8.85)
Carbonaceous fraction [g g^{-1} of PM[a]]				
OM	0.229 (±0.047)	0.174 (±0.123)	0.121 (±0.015)	0.469 (±0.082)
EC	0.007 (±0.006)	0.086 (±0.061)	0.063 (±0.008)	0.158 (±0.028)
Main inorganic fractions [g g^{-1} of PM[a]]				
Sulfate (SO$_4^{2-}$)	0.336 (±0.065)	0.284 (±0.163)	0.039 (±0.005)	0.063 (±0.001)
Nitrate (NO$_3^-$)	0.032 (±0.017)	0.019 (±0.006)	0.006 (±0.001)	0.016 (±0.002)
Ammonium (NH$_4^+$)	0.082 (±0.036)	0.090 (±0.064)	<lq	0.006 (±0.001)
Sodium (Na)	0.009 (±0.002)	0.018 (±0.012)	0.004 (±0.003)	0.003 (±0.001)
Soluble (Na$^+$)	*0.009 (±0.002)*	*<lq*	*0.001 (±0.001)*	*0.003 (±0.001)*
Potassium (K)	0.001 (±0.001)	0.013 (±0.001)	0.001 (±0.001)	0.001 (±0.001)
Soluble (K$^+$)	*<lq*	*<lq*	*<lq*	*0.001 (±0.001)*
Magnesium (Mg)	0.009 (±0.003)	0.012 (±0.004)	0.036 (±0.01)	0.010 (±0.001)
Soluble (Mg^{2+})	*0.006 (±0.001)*	*0.003 (±0.001)*	*0.003 (±0.001)*	*0.002 (±0.001)*
Calcium (Ca)	0.123 (±0.021)	0.208 (±0.015)	0.558 (±0.051)	0.142 (±0.010)
Soluble (Ca^{2+})	*0.123 (±0.021)*	*0.112 (±0.045)*	*0.293 (±0.03)*	*0.071 (±0.006)*
Others trace elements [mg g^{-1} of PM[a]]	174.1 (±41.49)	93.73 (±62.14)	171.9 (±31.9)	133.3 (±29.35)

Notes: <lq: below quantification limits which means that the concentration obtained for both downwind and the upwind site are not significantly different.
[a] PM$_{2.5}$ represents the sum of the aerosol major fractions concentrations (OM, EC, Sulfate, Nitrate, Ammonium and trace elements). An OM-to-OC conversion ratio of 1.2 was used.

Table 3
Trace element contributions to primary $PM_{2.5}$ (average (standard deviation)).

	Complex 1 Cast iron converter complex	Complex 2 Ore iron converter complex	Complex 3 Blast furnace slag storage area	Complex 4 Ore terminal
Other trace elements [mg g^{-1} of PM[a]]				
Al	5.904 (±5.113)	12.26 (±8.67)	29.08 (±8.71)	125.7 (±28.44)
As	0.197 (±0.054)	0.165 (±0.085)	0.019 (±0.003)	0.024 (±0.002)
Ba	0.106 (±0.047)	0.173 (±0.054)	0.218 (±0.064)	0.239 (±0.039)
Cd	0.035 (±0.011)	0.058 (±0.010)	0.009 (±0.002)	0.002 (±0.001)
Ce	3.600 (±3.107)	0.019 (±0.013)	0.022 (±0.004)	0.053 (±0.006)
Co	<lq	0.020 (±0.002)	0.018 (±0.005)	0.012 (±0.001)
Cr	0.355 (±0.048)	0.157 (±0.043)	0.317 (±0.109)	0.371 (±0.081)
Cs	<lq	0.040 (±0.029)	<lq	<lq
Cu	0.162 (±0.083)	0.827 (±0.346)	0.122 (±0.033)	0.152 (±0.01)
Fe	146.0 (±26.17)	70.07 (±49.55)	124.4 (±18.92)	2.205 (±0.241)
La	3.356 (±2.901)	<lq	0.013 (±0.002)	0.017 (±0.001)
Li	0.007 (±0.006)	0.018 (±0.013)	0.011 (±0.004)	0.008 (±0.001)
Mn	4.203 (±0.951)	2.875 (±0.680)	10.63 (±2.49)	1.412 (±0.223)
Mo	0.022 (±0.019)	0.303 (±0.187)	0.002 (±0.002)	0.019 (±0.002)
Ni	0.135 (±0.035)	0.161 (±0.015)	0.051 (±0.010)	0.050 (±0.003)
Pb	1.257 (±0.531)	2.315 (±0.394)	0.267 (±0.115)	0.158 (±0.014)
Rb	0.015 (±0.009)	0.206 (±0.087)	0.009 (±0.003)	0.013 (±0.001)
Sb	0.023 (±0.011)	<lq	0.007 (±0.001)	0.006 (±0.001)
Sc	<lq	<lq	0.016 (±0.005)	0.019 (±0.003)
Se	0.049 (±0.008)	0.111 (±0.052)	0.001 (±0.001)	<lq
Sn	0.184 (±0.025)	0.131 (±0.093)	0.026 (±0.012)	0.025 (±0.001)
Sr	0.029 (±0.025)	0.127 (±0.046)	0.293 (±0.055)	0.179 (±0.018)
Ti	0.952 (±0.112)	0.740 (±0.523)	4.686 (±0.693)	1.533 (±0.101)
Tl	<lq	0.028 (±0.020)	<lq	<lq
V	0.104 (±0.008)	0.097 (±0.006)	0.293 (±0.074)	0.250 (±0.073)
Zn	7.297 (±2.212)	2.788 (±1.223)	1.380 (±0.599)	0.755 (±0.074)
Zr	0.027 (±0.007)	0.037 (±0.001)	0.033 (±0.007)	0.111 (±0.022)

Notes: <lq: below quantification limits which means that the concentration obtained for both downwind and the upwind site are not significantly different.
[a] $PM_{2.5}$ represents the sum of the aerosol major fractions concentrations (OM, EC, Sulfate, Nitrate, Ammonium and trace elements). An OM-to-OC conversion ratio of 1.2 was used.

0.208 ± 0.015 g g^{-1}, 0.558 ± 0.051 g g^{-1} and 0.142 ± 0.010 g g^{-1} for complex 1, 2, 3 and 4, respectively. A global contamination of the metallurgic complex by resuspension processes from the slag storage area may partly explain this result, but significant differences are observed between complexes regarding the solubility of the calcium. While the soluble fraction (Ca^{2+}) represents 100% of the total calcium for complex 1, it drops to less than 53% for complex 2 (53%), 3 (52%) and 4 (50%), suggesting the influence of at least two distinct sources for this element.

3.3. Trace elements

All sources are characterized by a high contribution of trace elements (Table 3) representing 174.1 mg g^{-1}, 93.73 mg g^{-1}, 171.9 mg g^{-1} and 133.3 mg g^{-1} respectively for the complexes 1, 2, 3 and 4.

For the cast iron converter complex (complex 1), $PM_{2.5}$ are mainly enriched with iron (146.0 mg g^{-1}). Iron makes up 84% of the total traces elements (not including Ca) emitted by this source. To a lesser extent, we observed a significant contribution of zinc (Zn, 7.297 mg g^{-1}), aluminum (Al, 5.904 mg g^{-1}), manganese (Mn, 4.203 mg g^{-1}), titanium (Ti, 0.952 mg g^{-1}), cerium (Ce, 3.600 mg g^{-1}) and lanthanum (La, 3.356 mg g^{-1}). Zn represents 4% of the total traces elements followed by Al and Mn with respectively 3% and 2%. Ti, Ce and La represent each less than 2% of the total trace elements (not including Ca).

For the iron ore converter complex (complex 2), as for the complex 1, the main trace element emitted is Fe (70.07 mg g^{-1}) representing 74% of the total trace elements contribution (not including Ca). Also significant contribution of Al (12.26 mg g^{-1}), Mn (2.875 mg g^{-1}), Zn (2.788 mg g^{-1}) and Ti (0.704 mg g^{-1}) are observed. The main difference when comparing with complex 1, is an additional influence of lead (Pb) and copper (Cu) contributing to

2.315 mg g^{-1} (2% of the total trace elements) and 0.827 mg g^{-1} (less than 1% of the total traces elements), respectively.

Blast furnace slag storage area (complex 3) emissions are also characterized by high concentration of Fe (124.4 mg g^{-1}), Al (29.08 mg g^{-1}), Mn (10.63 mg g^{-1}) and Zn (1.380 mg g^{-1}). These metals represent 72% (Fe), 16% (Al), 6% (Mn) and less than 1% (Zn) of the total trace elements measured. The contribution of Ti is, for this source, higher than those determined for the other sources. Titanium represents 3% (4.686 mg g^{-1}) of the total trace elements emitted by complex 3.

The emission of the ore terminal (complex 4) are clearly dominated by Al which represents 94% of the total trace element emitted, with a contribution to $PM_{2.5}$ of 125.7 mg g^{-1} (Table 3). This contribution if four time higher than those observed for the others sources. The second more abundant trace element is Fe with contribution of 2.205 mg g^{-1} followed by Mn (1.412 mg g^{-1}) and Ti (1.533 mg g^{-1}).

3.4. Organic markers

Organic markers contributions are reported in Table 4. Note that only compounds or families of compounds showing a significant enrichment for at least one complex are reported. Overall, $PM_{2.5}$ enrichments with organic markers are very low. No significant $PM_{2.5}$ enrichment with any of the organic markers analyzed here is observed for the blast furnace slag storage area (complex 3). For complex 1 only a slight enrichment with light n-alkanes (C20-C28), hopanes and some PAHs can be detected, although it most likely reflects the influence of fuel combustion (handling vehicle, for instance) in the immediate surroundings of the source.

The most remarkable feature is related to the iron ore converter complex (complex 2) for which a contribution of 2.2 mg g^{-1} for PAHs is observed, corresponding to 1.3% of the OM emitted. Such

Table 4
Polycyclic Aromatic Hydrocarbon (PAHs), Sulfur PAHs, n-Alkanes and hopanes contributions to primary $PM_{2.5}$ (average (standard deviation)).

	Complex 1 Cast iron converter complex	**Complex 2** Ore iron converter complex	**Complex 3** Blast furnace slag storage area	**Complex 4** Ore terminal
Polycyclic Aromatic Hydrocarbons [mg g^{-1} of PM[a]]				
Phenanthrene	<lq	0.034 (±0.024)	<lq	0.016 (±0.001)
Anthracene	<lq	0.009 (±0.007)	<lq	0.002 (±0.001)
Fluoranthene	0.011 (±0.006)	0.399 (±0.164)	<lq	<lq
Acephenanthrene	<lq	0.024 (±0.017)	<lq	0.040 (±0.008)
Pyrene	<lq	0.178 (±0.097)	<lq	0.021 (±0.002)
Benzo[a]anthracene	<lq	0.155 (±0.101)	<lq	0.009 (±0.001)
Chrysene/ triphenylene	0.014 (±0.012)	0.258 (±0.153)	<lq	0.032 (±0.003)
benzo[b,k]fluoranthene	<lq	0.191 (±0.113)	<lq	0.010 (±0.003)
benzo[j]fluoranthene	<lq	0.022 (±0.015)	<lq	0.001 (±0.001)
benzo[e]pyrene	0.006 (±0.003)	0.219 (±0.155)	<lq	0.018 (±0.001)
benzo[a]pyrene	0.020 (±0.017)	0.178 (±0.108)	<lq	0.008 (±0.001)
Indeno[1,2,3 − cd]fluoranthene	0.023 (±0.020)	<lq	<lq	<lq
Indeno[1,2,3 - cd]pyrene	0.037 (±0.032)	0.251 (±0.148)	<lq	0.004 (±0.003)
Dibenzo[a,h]anthracene	0.031 (±0.027)	0.147 (±0.092)	<lq	0.005 (±0.001)
Benzo[g,h,i]perylene	0.047 (±0.041)	0.222 (±0.127)	<lq	0.013 (±0.001)
Sulfur PAH [mg g^{-1} of PM[a]]				
Benzo[b]naphtha(2,1-d)thiophene	0.002 (±0.001)	0.068 (±0.034)	<lq	0.014 (±0.001)
Benzo[b]naphtha(1,2-d)thiophene	<lq	0.011 (±0.008)	<lq	0.002 (±0.001)
Benzo[b]naphtha(2,3-d)thiophene	<lq	0.021 (±0.015)	<lq	0.002 (±0.001)
n-Alkanes [mg g^{-1} of PM[a]]				
n-Octadecane (C18)	0.320 (±0.277)	<lq	<lq	0.070 (±0.035)
n-Nonadecane (C19)	0.104 (±0.090)	0.056 (±0.040)	<lq	0.026 (±0.010)
n-Eicosane (C20)	0.156 (±0.099)	0.064 (±0.045)	<lq	0.034 (±0.017)
n-Heneicosane (C21)	0.096 (±0.045)	0.032 (±0.023)	<lq	0.031 (±0.008)
n-Docosane (C22)	0.259 (±0.152)	<lq	<lq	0.045 (±0.007)
n-Tricosane(C23)	0.124 (±0.086)	<lq	<lq	0.042 (±0.001)
n-Tetracosane (C24)	0.202 (±0.127)	<lq	<lq	0.042 (±0.003)
n-Pentacosane (C25)	0.287 (±0.209)	<lq	<lq	0.057 (±0.003)
n-Hexacosane (C26)	0.216 (±0.137)	<lq	<lq	0.045 (±0.003)
n-Heptacosane (C27)	0.448 (±0.343)	<lq	<lq	0.085 (±0.002)
n-Octacosane (C28)	0.134 (±0.097)	<lq	<lq	0.032 (±0.002)
n-Nonacosane (C29)	0.438 (±0.380)	0.093 (±0.066)	<lq	0.123 (±0.010)
n-Triacontane (C30)	0.055 (±0.047)	<lq	<lq	0.023 (±0.005)
n-Untricontane (C31)	0.400 (±0.298)	<lq	<lq	<lq
n-Dotriacontane (C32)	0.036 (±0.031)	<lq	<lq	0.008 (±0.006)
n-Tritriacontane (C33)	0.094 (±0.081)	<lq	<lq	0.026 (±0.010)
n-Tetratriacontane (C34)	<lq	0.131 (±0.093)	<lq	0.007 (±0.005)
n-Pentatriacontane (C35)	<lq	<lq	<lq	0.005 (±0.004)
n-Hexatriacontane (C36)	<lq	<lq	<lq	<lq
Hopanes [mg g^{-1} of PM[a]]				
17α(H)-trisnorhopane (H28)	0.014 (±0.008)	0.007 (±0.003)	<lq	0.004 (±0.001)
17α(H)-21β(H)-norhopane (H29)	0.019 (±0.008)	0.013 (±0.002)	<lq	0.010 (±0.001)
17α(H)-21β(H)-hopane (H30)	0.011 (±0.007)	<lq	<lq	0.011 (±0.001)
22S,17α(H)-21β(H)-homohopane (S-H31)	0.016 (±0.014)	<lq	<lq	0.005 (±0.001)
22R,17α(H)-21β(H)-homohopane (R-H31)	0.013 (±0.011)	0.005 (±0.003)	<lq	0.006 (±0.004)
22S,17α(H)-21β(H)-bishomohopane (S-H32)	<lq	0.006 (±0.004)	<lq	0.004 (±0.001)
22R,17α(H)-21β(H)-Bishomohopane (R-H32)	0.012 (±0.006)	0.008 (±0.006)	<lq	0.005 (±0.001)
22S,17α(H)-21β(H)-Trishomohopane (S-H33)	0.009 (±0.004)	<lq	<lq	0.002 (±0.002)
22R,17α(H)-21β(H)-Trishomohopane (R-H33)	<lq	0.004 (±0.003)	<lq	<lq

Notes: <lq: below quantification limits which means that the concentration obtained for both downwind and the upwind site are not significantly different.

[a] $PM_{2.5}$ represents the sum of the aerosol major fractions concentrations (OM, EC, Sulfate, Nitrate, Ammonium and trace elements). An OM-to-OC conversion ratio of 1.2 was used.

contribution of PAHs to OM is more than 10 times higher than what is typically observed in urban environments (El Haddad et al., 2011; Manoli et al., 2016). The total PAHs concentration is dominated by fluoranthene (0.399 mg g^{-1}), chrysene/triphene (0.258 mg g^{-1}), indeno[1,2,3 - cd]pyrene (0.251 mg g^{-1}), benzo-ghi-perylene (0.222 mg g^{-1}) and benzo-e-pyrene (0.219 mg g^{-1}). Benzo-a-pyrene is also significantly emitted (0.178 mg g^{-1}). Also, we observe significant $PM_{2.5}$ enrichments with sulfur-containing PAHs (SPAHs) dominated by benzo[b]naphtha(2,1-d)thiophene (0.068 mg g^{-1}), benzo[b]naphtha(1,2-d)thiophene (0.011 mg g^{-1})

and benzo[b]naphtha(2,3-d)thiophene (0.021 mg g^{-1}). These compounds were not detected at the upwind site but only at the downwind site. They are thus exclusively emitted by sources located in between. Thiophenes are only very sparsely reported in the literature. They are naturally present in coal, crude oil and oil shale (Andersson and Schmid, 1995; Chou, 2012; Grimmer et al., 1983) and are mainly emitted by combustion sources using high sulfur containing fuels such as coal (Lee et al., 2005; Stefanova et al., 2002; Thuß et al., 2000) or oil derived products (Wang et al., 2007). They have also recently been reported in graphite material
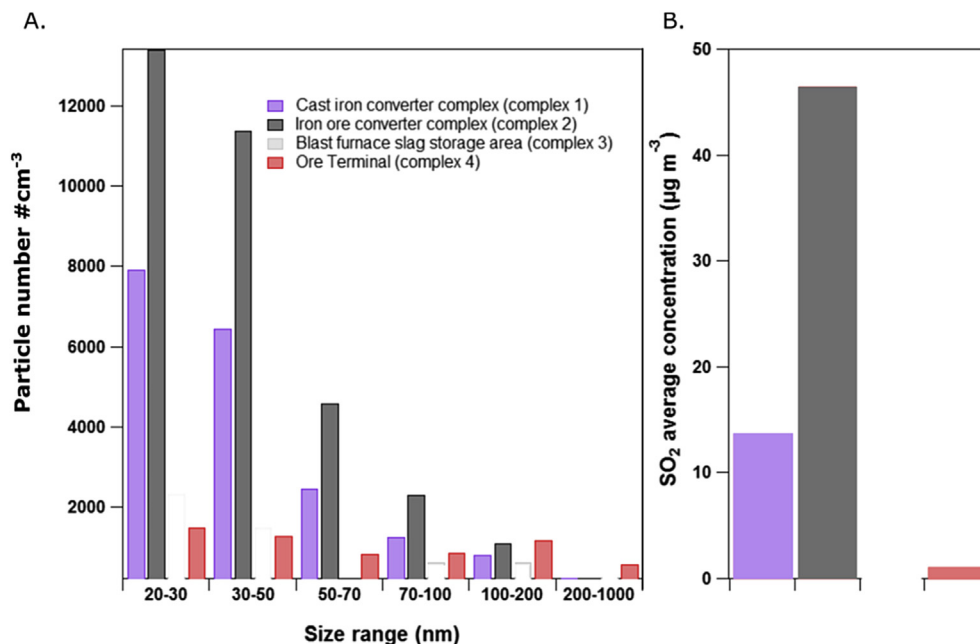
Fig. 2. (2-column fitting image): A. average particle number size distribution measured downwind of each industrial complex during filter sampling periods and B. average SO$_2$ concentrations measured downwind of each industrial complex during filter sampling periods.

production industrial environments (Golly et al., 2015).

PAHs, SPAHs and n-alcanes are observed as well in emissions of the ore terminal (complex 4). However, their contributions are not as significant as those reported for complex 2. These enrichments can be due, as for OC and EC, to the ore, especially to the petroleum coke and coal, stored in this area.

4. Discussion

Results show that the emissions from complex 1 are characterized by ultrafine particles (particles with size under 100 nm) associated to PM$_{2.5}$ enrichments with SO$_4^{2-}$, OM, Ca, Fe, Al, Zn, Mn, Ti, Ce, La. The complex 1 gathers all the in-ladle metallurgic treatment installation and the oxygen converters. Basic oxygen furnace is the main industrial process operating in this complex. The aim of this process is to eliminate, by oxidation, the last 4% of carbon impurities of the iron cast, which can explain the significant PM$_{2.5}$ enrichment with OM not associated with any significant EC fraction. The enrichments observed with all of trace elements characterized here are also in agreement with materials used in the complex 1. The high enrichment with Fe was expected because of the smelting process of the iron cast (constituted by about 96% of Fe). Lime (CaO) is also used to eliminate phosphor, silicon and manganese from the iron cast and represents most probably the main sources of Ca from complex 1. Observed in lower proportion, the presence of trace elements such as Al, Zn, Mn or Ti can possibly be explained by impurities within the iron ore. In addition, Ce can be used to reduce the sulfate and oxides content in steel while La can be used to improve the resistance of stainless steel. Our results are in agreement with those obtained by Larsen et al. (2008) which studied the emissions from a basic oxygen furnace. However, the proportions between the emitted species are sensibly different. For example, the Ca-to-Fe ratio obtained by Larsen et al. (2008) is 6 times higher than the one observed here. These differences can be explained by the difference of the particle sizes fraction considered (PM$_{2.5}$ here and TSP for Larsen et al., 20018) and by processes involved.

The complex 2 is characterized by the emission of SO$_4^{2-}$, OM, EC, Ca, Fe, Al, Mn, Zn, Ti, Pb, Cu, PAH, SPAH and ultrafine particles. The cast iron is produced in the complex 2 from the fusion of iron ore, using coke as fuel. The emission of ultrafine particles associated with SO$_2$, and the enrichment with SO$_4^{2-}$, OM, EC, PAH and SPAH observed, are in agreement with the combustion processes occurring in the complex 2 (coke plant, sinter plant and blast furnace). PAHs are mainly emitted by combustion sources (Ravindra et al., 2008) and several studies have already highlighted the high contribution of industrial sources, especially steel and coke industries, to the ambient PAHs concentrations (El Haddad et al., 2011, 2013; Khalili et al., 1995; Yang et al., 1998, 2002). The complex 2 is the only one in which combustions sources occur. High emissions of PAHs were therefore expected. The abundance of SPAHs is most probably linked to the use of high sulfur containing fuels used. Results obtained here confirm the relevance of PAHs and SPAHs in terms of source markers of steel production activities and more precisely coke plant emissions. The contribution of all traces elements (Ca, Fe, Al, Mn, Zn, Ti, Pb, Cu) are also in agreement with the emission of coal and coke combustions (Li et al., 2006; Linak et al., 2007). Contribution of Fe can also be enhanced by the use of iron ore (magnetite and hematite) to produce the cast iron in the sinter plant. Furthermore, traces of Al, Mn, Zn and Ti can also be found in these iron ores. Enrichments determined for all trace elements are also in agreement with previous studies. Previous works (Mohiuddin et al., 2014; Moreno et al., 2004) showed high contribution of Pb and Cu but also of Al, Fe, Zn, Mg and Mn on three sampling sites under blast furnace plant's influence. Lime (CaO) or calcium carbide (CaC$_2$) are typically used during the blast furnace operations for desulfurization purposes, which probably explains the high enrichment observed with Ca. However, AToFMS measurements carried out in the vicinity of a steel plant in the UK (Dall' Osto et al., 2008) showed that fine metals-rich particles were not associated to Ca, indicating that Ca and metals (mostly Fe) are not internally mixed and are most probably emitted by different processes. As for Ca, Ti emissions can also be explained by the desulfurization process since ferrotitanium is often used as cleansing

agent for steel plant emissions (Pokorná et al., 2015). Fugitive emissions can also result from hot and cold rolling processes and emissions from cooling towers, which may results in diffuse emissions of trace elements that are dissolved in water and mostly Ca, Mg. In agreement with our results, high contribution of Fe, OC, EC, SO_4^{2-}, Zn and Al were already observed for blast furnace emissions (Larsen et al., 2008). However, as for complex 1, the proportions between species are significantly different from those reported by Larsen et al. (2008). Furthermore, no calcium enrichment was observed in the study carried out by Larsen et al. (2008). These discrepancies can be explained by the difference of particle size fraction considered or, most likely, by the additional sources and processes involved in our study (blast furnace but also coking plant and sinter plant).

The blast furnace slag storage area (complex 3) is also characterized by emissions of Ca, Fe, Al, Mn and Zn. The main emission process involved here is the resuspension of blast furnace slag materials. Blast furnace slag is mainly composed with various oxides of iron, calcium, titanium, manganese, magnesium and aluminum (Dimitrova, 1996; Haha et al., 2011, 2012) as well as calcium sulfate ($CaSO_4$) and calcium sulfide (CaS). Furthermore, part of the stocked wastes is derived from combustion processes (blast furnace process, mainly) which probably explains the significant contribution of EC.

The ore terminal (complex 4) emissions are mainly characterized by the abundance of OM, EC, Ca, Al, Fe, Mn, Ti, PAHs and SPAHs. As for complex 3, the main emission process involved is the resuspension of ore and of the various materials stored. The main materials stored inside the complex 4 are lime, coal, petroleum coke, bauxite and alumina (Al_2O_3). The abundance of OM, EC, PAHs and SPAHs are most probably related to the resuspension of petroleum coke and coal and the abundance of Ca by the resuspension of lime. As the petroleum coke is a produced by thermal cracking, ash is one sub product of coke and represent typically between 1 and 2% of the total coke mass (Bryers, 1995). Petroleum coke ashes are mainly composed of Ca, Fe, Al, Mg which can explain the contribution of these species observed here (Bryers, 1995). However, conversely to the others complexes, all these traces elements exhibit lower contributions than Aluminum. The contribution of Al is 4 times higher than those determined for the others complexes. Bauxite and alumina (Al_2O_3) stored in the ore terminal explain, most probably, the very high emissions of Al.

5. Conclusion

We report 4 chemical emission profiles of $PM_{2.5}$, obtained with an enrichment based approach, for the conversion processes of the cast iron (complex 1), the conversion processes of the iron ore (complex 2), and for 2 storage areas (blast furnace slag area -complex 3- and an ore terminal -complex 4-). The enrichment based approach allows the characterization of both stack and fugitive emissions. The approach also takes into consideration the non-continuous nature of many steelmaking processes. Considering the wide number of parameters able to modify the chemical fingerprints of the emissions (steel industry activities, meteorology), enrichments were found to be very consistent for all the pairs of samples selected for a given source.

As expected, the $PM_{2.5}$ chemical source profiles obtained for the storage area (blast furnace slags and ore) reflect the chemical nature of the stored materials. The atmospheric life time of such coarse particles limits their ability to be transported over long distances, but the global enrichments observed for the $PM_{2.5}$ fraction, which reached 50 μg m^{-3}, show that such sources cannot be neglected for source apportionment exercises.

The steelmaking activities (complexes 1 and 2) are on the

contrary characterized by the abundance of ultrafine particles (Dp < 100 nm) associated with OC, SO_4^{2-}, Ca, Fe, Al, Zn, Mn, La and Ce. Important contribution of PAHs and SPAHs are also observed for the complex 2, which merges the activities of the coke plant, the sinter plant and the blast furnaces. For both complexes 1 and 2, sulfates are only partially neutralized by ammonium suggesting the emission of acidic particles. However, the large fraction of soluble calcium and its potential association, at least partial, with sulfate ($CaSO_4$) in the emissions, could reduce this deficit of cations. Calcium is also widely used as a proxy of the dust contributions in source apportionments studies. Our results suggest that this assumption should be reexamined in environments impacted by industrial emission.

Appendix A. Supplementary data

Supplementary data related to this article can be found at http://dx.doi.org/10.1016/j.atmosenv.2016.12.032.

References

Aiken, A.C., Decarlo, P.F., Kroll, J.H., Worsnop, D.R., Huffman, J.A., Docherty, K.S., Ulbrich, I.M., Mohr, C., Kimmel, J.R., Sueper, D., Sun, Y., Zhang, Q., Trimborn, A., Northway, M., Ziemann, P.J., Canagaratna, M.R., Onasch, T.B., Alfarra, M.R., Prevot, A.S.H., Dommen, J., Duplissy, J., Metzger, A., Baltensperger, U., Jimenez, J.L., 2008. O/C and OM/OC ratios of primary, secondary, and ambient organic aerosols with high-resolution time-of-flight aerosol mass spectrometry. Environ. Sci. Technol. 42 (12), 4478–4485. http://dx.doi.org/10.1021/es703009q.

Alleman, L.Y., Lamaison, L., Perdrix, E., Robache, A., Galloo, J.C., 2010. PM10 metal concentrations and source identification using positive matrix factorization and wind sectoring in a French industrial zone. Atmos. Res. 96 (4), 612–625. http://dx.doi.org/10.1016/j.atmosres.2010.02.008.

Andersson, J.T., Schmid, B., 1995. Polycyclic aromatic sulfur heterocycles IV. Determination of polycyclic aromatic compounds in a shale oil with the atomic emission detector. J. Chromatogr. A 693 (2), 325–338. http://dx.doi.org/10.1016/0021-9673(94)01111-Q.

Aymoz, G., Jaffrezo, J.-L., Chapuis, D., Cozic, J., Maenhaut, W., 2007. Seasonal variation of PM10 main constituents in two valleys of the French Alps. I: EC/OC fractions. Atmos. Chem. Phys. Discuss. 7, 661–675. http://dx.doi.org/10.5194/acpd-6-6211-2006.

Baraniecka, J., Pyrzyńska, K., Szewczyńska, M., Pośniak, M., Dobrzyńska, E., 2010. Emission of polycyclic aromatic hydrocarbons from selected processes in steelworks. J. Hazard. Mat. 183 (1–3), 111–115. http://dx.doi.org/10.1016/j.jhazmat.2010.06.120.

Bryers, R.W., 1995. Utilization of petroleum coke and petroleum coke/coal blends as a means of steam raising. Fuel Process. Technol. 44 (1–3), 121–141. http://dx.doi.org/10.1016/0378-3820(94)00118-D.

Buonanno, G., Stabile, L., Avino, P., Belluso, E., 2011. Chemical, dimensional and morphological ultrafine particle characterization from a waste-to-energy plant. Waste Manag. 31 (11), 2253–2262. http://dx.doi.org/10.1016/j.wasman.2011.06.017.

Ben Haha, M., Lothenbach, B., Le Saout, G., Winnefeld, F., 2011. Influence of slag chemistry on the hydration of alkali-activated blast-furnace slag — Part I: effect of MgO. Cem. Concr. Res. 41, 955–963.

Ben Haha, M., Lothenbach, B., Le Saout, G., Winnefeld, F., 2012. Influence of slag chemistry on the hydration of alkali-activated blast-furnace slag — Part II: effect of Al2O3. Cem. Concr. Res. 42 (1), 74–83. http://dx.doi.org/10.1016/j.cemconres.2011.08.005.

Canonaco, F., Crippa, M., Slowik, J.G., Baltensperger, U., Prévôt, A.S.H., 2013. SoFi, an IGOR-based interface for the efficient use of the generalized multilinear engine (ME-2) for the source apportionment: ME-2 application to aerosol mass spectrometer data. Atmos. Meas. Tech. 6, 3649–3661. http://dx.doi.org/10.5194/amt-6-3649-2013.

Cavalli, F., Viana, M., Yttri, K.E., Genberg, J., Putaud, J.-P., 2010. Toward a standardised thermal-optical protocol for measuring atmospheric organic and elemental carbon: the EUSAAR protocol. Atmos. Meas. Tech. 3, 79–89. http://dx.doi.org/10.5194/amt-3-79-201.

Chen, B., Stein, A.F., Maldonado, P.G., Sanchez de la Campa, A.M., Gonzalez-

Castanedo, Y., Castell, N., de la Rosa, J.D., 2013. Size distribution and concentrations of heavy metals in atmospheric aerosols originating from industrial emissions as predicted by the HYSPLIT model. Atmos. Environ. 71, 234–244. http://dx.doi.org/10.1016/j.atmosenv.2013.02.013.

Chou, C.L., 2012. Sulfur in coals: a review of geochemistry and origins. Int. J. Coal Geol. 100, 1–13. http://dx.doi.org/10.1016/j.coal.2012.05.009.

Dall'Osto, M., Booth, M.J., Smith, W., Fisher, R., Harrison, R.M., 2008. A study of the size distributions and the chemical characterization of airborne particles in the vicinity of a large integrated steelworks. Aerosol Sci. Technol. 42 (12), 981–991. http://dx.doi.org/10.1080/02786820802339587.

Dimitrova, S.V., 1996. Metal sorption on blast-furnace slag. Water Res. 30 (1), 228–232. http://dx.doi.org/10.1016/0043-1354(95)00104-S.

Golly, B., Brulfert, G., Berlioux, G., Jaffrezo, J.-L., Besombes, J.-L., 2015. Large chemical characterisation of PM emitted from graphite material production: application in source apportionment. Sci. Total Environ. 538, 634–643. http://dx.doi.org/10.1016/j.scitotenv.2015.07.115.

Grimmer, G., Jacob, J., Naujack, K.-W., 1983. Profile of the polycyclic aromatic compounds from crude oils. Anal. Chem. 314, 29–36. http://dx.doi.org/10.1007/BF00476507.

Guinot, B., Gonzalez, B., De Faria, J.P., Kedia, S., 2016. Particuology Particulate matter characterization in a steelworks using conventional sampling and innovative lidar observations. Particuology 28, 43–51. http://dx.doi.org/10.1016/j.partic.2015.10.002.

El Haddad, I., D'Anna, B., Temime-Roussel, B., Nicolas, M., Boreave, A., Favez, O., Voisin, D., Sciare, J., George, C., Jaffrezo, J.L., Wortham, H., Marchand, N., 2013. Towards a better understanding of the origins, chemical composition and aging of oxygenated organic aerosols: case study of a Mediterranean industrialized environment, Marseille. Atmos. Chem. Phys. 13, 7875–7894. http://dx.doi.org/10.5194/acp-13-7875-2013.

El Haddad, I., Marchand, N., Dron, J., Temime-Roussel, B., Quivet, E., Wortham, H., Jaffrezo, J.L., Baduel, C., Voisin, D., Besombes, J.L., Gille, G., 2009. Comprehensive primary particulate organic characterization of vehicular exhaust emissions in France. Atmos. Environ. 43, 6190–6198. http://dx.doi.org/10.1016/j.atmosenv.2009.09.001.

El Haddad, I., Marchand, N., Wortham, H., Piot, C., Besombes, J.L., Cozic, J., Chauvel, C., Armengaud, A., Robin, D., Jaffrezo, J.L., 2011. Primary sources of PM2.5organic aerosol in an industrial Mediterranean city, Marseille. Atmos. Chem. Phys. 11 (5), 2039–2058. http://dx.doi.org/10.5194/acp-11-2039-2011.

Hleis, D., Fernández-Olmo, I., Ledoux, F., Kfoury, A., Courcot, L., Desmonts, T., Courcot, D., 2013. Chemical profile identification of fugitive and channeled particle emissions from an integrated iron and steelmaking plant. J. Hazard. Mat. 250–251, 246–255. http://dx.doi.org/10.1016/j.jhazmat.2013.01.080.

Jaffrezo, J.L., Calas, N., Bouchet, M., 1998. Carboxylic acids measurements with ionic chromatography. Atmos. Environ. 32, 2705–2708. http://dx.doi.org/10.1016/S1352-2310(98)00026-0.

Kfoury, A., Ledoux, F., Roche, C., Delmaire, G., Roussel, G., Courcot, D., 2016. PM2.5 source apportionment in a French urban coastal site under steelworks emission influences using constrained non-negative matrix factorization receptor model. J. Environ. Sci. 40, 114–128. http://dx.doi.org/10.1016/j.jes.2015.10.025.

Khalili, N.R., Scheff, P.A., Holsen, T.M., 1995. PAH source fingerprints for coke ovens, diesel and, gasoline engines, highway tunnels, and wood combustion emissions. Atmos. Environ. 29 (4), 533–542. http://dx.doi.org/10.1016/1352-2310(94)00275-P.

Larsen, B.R., Junninen, H., Mønster, J., Viana, M., Tsakovski, P., Duvall, R.M., Norris, G., Querol, X., 2008. The Krakow Receptor Modelling Inter-comparison Exercise.

Lee, R.G.M., Coleman, P., Jones, J.L., Jones, K.C., Lohmann, R., 2005. Emission factors and importance of PCDD/Fs, PCBs, PCNs, PAHs and PM 10 from the domestic burning of coal and wood in the U.K. Environ. Sci. Technol. 39 (6), 1436–1447. http://dx.doi.org/10.1021/es048745i.

Leoni, C., Hovorka, J., Dočekalová, V., Cajthaml, T., Marvanová, S., 2016. Source impact determination using airborne and ground measurements of industrial plumes. Environ. Sci. Technol. 50, 9881–9888. http://dx.doi.org/10.1021/acs.est.6b02304.

Li, F., Zhai, J., Fu, X., Sheng, G., 2006. Characterization of fly ashes from circulating fluidized bed combustion (CFBC) boilers cofiring coal and petroleum coke. Energy & Fuels 20 (14), 1411–1417.

Lim, J.-M., Lee, J.-H., Moon, J.-H., Chung, Y.-S., Kim, K.-H., 2010. Airborne PM10 and metals from multifarious sources in an industrial complex area. Atmos. Res. 96 (1), 53–64. http://dx.doi.org/10.1016/j.atmosres.2009.11.013.

Linak, W.P., Yoo, J.-I., Wasson, S.J., Zhu, W., Wendt, J.O.L., Huggins, F.E., Chen, Y., Shah, N., Huffman, G.P., Gilmour, M.I., 2007. Ultrafine ash aerosols from coal combustion: characterization and health effects. Proc. Combust. Inst. 31 (2), 1929–1937. http://dx.doi.org/10.1016/j.proci.2006.08.086.

Liu, G.Z., Berg, D.R., Vasys, V.N., Dettmann, M.E., Zielinska, B., Schauer, J.J., 2010. Analysis of C1, C2, and C10 through C33 particle-phase and semi-volatile organic compound emissions from heavy-duty diesel engines. Atmos. Environ. 44 (8), 1108–1115. http://dx.doi.org/10.1016/j.atmosenv.2009.11.036.

Lough, G.C., Christensen, C.G., Schauer, J.J., Tortorelli, J., Mani, E., Lawson, D.R., Clark, N.N., Gabele, P.A., 2007. Development of molecular marker source profiles for emissions from on-road gasoline and diesel vehicle fleets. J. Air Waste Manag. Assoc. 57 (10), 1190–1199. http://dx.doi.org/10.3155/1047-3289.57.10.1190.

Manoli, E., Kouras, A., Karagkiozidou, O., Argyropoulos, G., Voutsa, D., Samara, C., 2016. Polycyclic aromatic hydrocarbons (PAHs) at traffic and urban background sites of northern Greece: source apportionment of ambient PAH levels and PAH-induced lung cancer risk. Environ. Sci. Pollut. Res. 23, 3556–3568. http://dx.doi.org/10.1007/s11356-015-5573-5.

Mbengue, S., Alleman, L.Y., Flament, P., 2017. Metal-bearing fine particle sources in a coastal industrialized environment. Atmos. Res. J. 183, 202–211. http://dx.doi.org/10.1016/j.atmosres.2016.08.014.

Mohiuddin, K., Strezov, V., Nelson, P.F., Stelcer, E., Evans, T., 2014. Mass and elemental distributions of atmospheric particles nearby blast furnace and electric arc furnace operated industrial areas in Australia. Sci. Total Env. 487, 323–334. http://dx.doi.org/10.1016/j.scitotenv.2014.04.025.

Moreno, T., Merolla, L., Gibbons, W., Greenwell, L., Jones, T., Richards, R., 2004. Variations in the source, metal content and bioreactivity of technogenic aerosols: a case study from Port Talbot, Wales, UK. Sci. Total Environ. 333 (1–3), 59–73. http://dx.doi.org/10.1016/j.scitotenv.2004.04.019.

Nolte, C.G., Schauer, J.J., Cass, G.R., Simoneit, B.R.T., 1999. Highly polar organic compounds present in meat smoke. Environ. Sci. Technol. 33 (19), 3313–3316. http://dx.doi.org/10.1021/es990122v.

Nolte, C.G., Schauer, J.J., Cass, G.R., Simoneit, B.R.T., 2001. Highly polar organic compounds present in wood smoke and in the ambient atmosphere. Environ. Sci. Technol. 35 (10), 1912–1919. http://dx.doi.org/10.1021/es001420r.

Okamoto, S., Wangkiat, A., Pongkiatkul, P., Nakkhwan, C., Oanh, N.K., 2012. Comparative study on the CMB-8 and PMF models for a coastal industrial area. Int. J. Environ. Prot. 2, 1–6.

Paatero, P., Tapper, U., 1994. Positive matrix factorization - a nonnegative factor model with optimal utilization of error estimates of data values. Environmetrics 5, 111–126. http://dx.doi.org/10.1002/env.3170050203.

Pokorná, P., Hovorka, J., Klán, M., Hopke, P.K., 2015. Source apportionment of size resolved particulate matter at a European air pollution hot spot. Sci. Total Environ. 502, 172–183. http://dx.doi.org/10.1016/j.scitotenv.2014.09.021.

Ravindra, K., Sokhi, R., Van Grieken, R., 2008. Atmospheric polycyclic aromatic hydrocarbons: source attribution, emission factors and regulation. Atmos. Environ. 42 (13), 2895–2921. http://dx.doi.org/10.1016/j.atmosenv.2007.12.010.

Riffault, V., Arndt, J., Marris, H., Mbengue, S., Setyan, A., Alleman, L.Y., Deboudt, K., Flament, P., Augustin, P., Delbarre, H., Wenger, J., 2015. Fine and ultrafine particles in the vicinity of industrial activities: a review. Crit. Rev. Environ. Sci. Technol. 45 (21) http://dx.doi.org/10.1080/10643389.2015.1025636.

Robinson, A.L., Subramanian, R., Donahue, N.M., Bernardo-Bricker, A., Rogge, W.F., 2006a. Source apportionment of molecular markers and organic aerosol. 2. Biomass smoke. Environ. Sci. Technol. 40 (24), 7811–7819. http://dx.doi.org/10.1021/es060782h.

Robinson, A.L., Subramanian, R., Donahue, N.M., Bernardo-Bricker, A., Rogge, W.F., 2006b. Source apportionment of molecular markers and organic aerosol. 3. Food cooking emissions. Environ. Sci. Technol. 40 (24), 7820–7827. http://dx.doi.org/10.1021/es060781p.

Rogge, W.F., Hildemann, L.M., Mazurek, M.A., Cass, G.R., Simoneit, B.R., 1998. Sources of fine organic aerosol. 9. Pine, oak, and synthetic log combustion in residential fireplaces. Environ. Sci. Technol. 32 (1), 13–22. http://dx.doi.org/10.1021/es960930b.

Rogge, W.F., Hildemann, L.M., Mazurek, M.A., Cass, G.R., Simoneit, B.R.T., 1993a. Sources of fine organic aerosol. 2. Noncatalyst and catalyst-equipped automobiles and heavy-duty diesel trucks. Environ. Sci. Technol. 27 (4), 636–651. http://dx.doi.org/10.1021/es00041a007.

Rogge, W.F., Hildemann, L.M., Mazurek, M.A., Cass, G.R., Simoneit, B.R.T., 1993b. Sources of fine organic aerosol. 3. Road dust, tire debris, and organometallic brake lining dust: roads as sources and sinks. Environ. Sci. Technol. 27 (9), 1802–1904. http://dx.doi.org/10.1021/es00046a019.

Rogge, W.F., Hildemann, L.M., Mazurek, M.A., Cass, G.R., Simoneit, B.R.T., 1997a. Sources of fine organic aerosol. 7. Hot asphalt roofing tar pot fumes. Environ. Sci. Technol. 31 (10), 2726–2730. http://dx.doi.org/10.1021/es960525k.

Rogge, W.F., Hildemann, L.M., Mazurek, M.A., Cass, G.R., Simoneit, B.R.T., 1997b. Sources of fine organic aerosol. 8. Boilers burning no. 2 Distillate fuel oil. Environ. Sci. Technol. 31 (10), 2731–2737. http://dx.doi.org/10.1021/es9609563.

Rogge, W.F., Hildemann, L.M., Mazurek, M.A., Cass, G.R., Simonelt, B.R.T., 1991. Sources of fine organic aerosol .1. Charbroilers and meat cooking operations. Environ. Sci. Technol. 25 (6), 1112–1125. http://dx.doi.org/10.1021/es00018a015.

Sánchez de la Campa, A.M., de la Rosa, J.D., González-Castanedo, Y., Fernández-Camacho, R., Alastuey, A., Querol, X., Pio, C., 2010. High concentrations of heavy metals in PM from ceramic factories of Southern Spain. Atmos. Res. 96 (4), 633–644. http://dx.doi.org/10.1016/j.atmosres.2010.02.011.

Schauer, J.J., Kleeman, M.J., Cass, G.R., Simoneit, B.R.T., 1999a. Measurement of emissions from air pollution sources. 1. C1 through C29 organic compounds from meat charbroiling. Environ. Sci. Technol. 33 (10), 1566–1577. http://dx.doi.org/10.1021/es980076j.

Schauer, J.J., Kleeman, M.J., Cass, G.R., Simoneit, B.R.T., 1999b. Measurement of emissions from air pollution sources. 2. C1 through C30 organic compounds from medium duty diesel trucks. Environ. Sci. Technol. 33 (10), 1578–1587. http://dx.doi.org/10.1021/es980081n.

Schauer, J.J., Kleeman, M.J., Cass, G.R., Simoneit, B.R.T., 2001. Measurement of emissions from air pollution sources. 3. C1-C29 organic compounds from fireplace combustion of wood. Environ. Sci. Technol. 35 (9), 1716–1728. http://dx.doi.org/10.1021/es001331e.

Schauer, J.J., Kleeman, M.J., Cass, G.R., Simoneit, B.R.T., 2002a. Measurement of emissions from air pollution sources. 4. C1-C27 organic compounds from cooking with seed oils. Environ. Sci. Technol. 36 (4), 567–575. http://dx.doi.org/10.1021/es002053m.

Schauer, J.J., Kleeman, M.J., Cass, G.R., Simoneit, B.R.T., 2002b. Measurement of

emissions from air pollution sources. 5. C1-C32 organic compounds from gasoline-powered motor vehicles. Environ. Sci. Technol. 36 (6), 1169–1180. http://dx.doi.org/10.1021/es0108077.

Schauer, J.J., Rogge, W.F., Hildemann, L.M., Mazurek, M.A., Cass, G.R., Simoneit, B.R.T., 1996. Source apportionment of airborne particulate matter using organic compounds as tracers. Atmos. Environ. 30, 3837–3855. http://dx.doi.org/10.1016/1352-2310(96)00085-4.

Simoneit, B.R.T., Schauer, J.J., Nolte, C.G., Oros, D.R., Elias, V.O., Fraser, M.P., Rogge, W.F., Cass, G.R., 1999. Levoglucosan, a tracer for cellulose in biomass burning and atmospheric particles. Atmos. Environ. 33 (2), 173–182. http://dx.doi.org/10.1016/S1352-2310(98)00145-9.

Stefanova, M., Marinov, S.P., Mastral, A.M., Callén, M.S., Garcí, T., 2002. Emission of oxygen, sulphur and nitrogen containing heterocyclic polyaromatic compounds from lignite combustion. Fuel Process. Technol. 77–78, 89–94. http://dx.doi.org/10.1016/S0378-3820(02)00061-9.

Taiwo, A.M., Beddows, D.C.S., Calzolai, G., Harrison, R.M., Lucarelli, F., Nava, S., Shi, Z., Valli, G., Vecchi, R., 2014. Science of the Total Environment Receptor modelling of airborne particulate matter in the vicinity of a major steelworks site. Sci. Total Environ. 490, 488–500. http://dx.doi.org/10.1016/j.scitotenv.2014.04.118.

Thuß, U., Popp, P., Ehrlich, C., Kalkoff, W., 2000. Identification and quantification of thiaarenes in the flue gas of lignite-fired domestic heating. j. High resolut. Chromatogr 23, 457–473.

Tsai, J.H., Lin, K.H., Chen, C.Y., Ding, J.Y., Choa, C.G., Chiang, H.L., 2007. Chemical constituents in particulate emissions from an integrated iron and steel facility. J. Hazard. Mat. 147 (1–2), 111–119. http://dx.doi.org/10.1016/j.jhazmat.2006.12.054.

Viana, M., Pandolfi, M., Minguillón, M.C., Querol, X., Alastuey, a., Monfort, E., Celades, I., 2008. Inter-comparison of receptor models for PM source apportionment: case study in an industrial area. Atmos. Environ. 42 (16), 3820–3832. http://dx.doi.org/10.1016/j.atmosenv.2007.12.056.

Waked, a., Favez, O., Alleman, L.Y., Piot, C., Petit, J.E., Delaunay, T., Verlinden, E., Golly, B., Besombes, J.L., Jaffrezo, J.L., Leoz-Garziandia, E., 2014. Source apportionment of PM10 in a north-western Europe regional urban background site (Lens, France) using positive matrix factorization and including primary biogenic emissions. Atmos. Chem. Phys. 14, 3325–3346. http://dx.doi.org/10.5194/acp-14-3325-2014.

Wang, Z., Li, K., Lambert, P., Yang, C., 2007. Identification, characterization and quantitation of pyrogenic polycylic aromatic hydrocarbons and other organic compounds in tire fire products. J. Chromatogr. A 1139 (1), 14–26. http://dx.doi.org/10.1016/j.chroma.2006.10.085.

Weitkamp, E.A., Lipsky, E.M., Pancras, P.J., Ondov, J.M., Polidori, A., Turpin, B.J., Robinson, A.L., 2005. Fine particle emission profile for a large coke production facility based on highly time-resolved fence line measurements. Atmos. Environ. 39 (36), 6719–6733. http://dx.doi.org/10.1016/j.atmosenv.2005.06.028.

Yang, H.H., Lai, S.O., Hsieh, L.T., Hsueh, H.J., Chi, T.W., 2002. Profiles of PAH emission from steel and iron industries. Chemosphere 48 (10), 1061–1074. http://dx.doi.org/10.1016/S0045-6535(02)00175-3.

Yang, H.H., Lee, W.J., Chen, S.J., Lai, S.O., 1998. PAH emission from various industrial stacks. J. Hazard. Mat. 60 (2), 159–174. http://dx.doi.org/10.1016/S0304-3894(98)00089-2.

Yatkin, S., Bayram, A., 2008. Determination of major natural and anthropogenic source profiles for particulate matter and trace elements in Izmir, Turkey. Chemosphere 71 (4), 685–696. http://dx.doi.org/10.1016/j.chemosphere.2007.10.070.

Yoo, J.I., Kim, K.H., Jang, H.N., Seo, Y.C., Seok, K.S., Hong, J.H., Jang, M., 2002. Emission characteristics of particulate matter and heavy metals from small incinerators and boilers. Atmos. Environ. 36, 5057–5066. http://dx.doi.org/10.1016/S1352-2310(02)00557-5.

1
2

Steel production processes:

This facility is composed by 1 discharging quay, 1 sinter plant, 1 coke plant, 2 blast furnaces, 2 oxygen converters, 2 continuous casters, 1 in-ladle metallurgy treatment installation, 1 hot strip mill. The industrial processes used in this facility are not publicly available. However, the general steel manufacturing processes are known. Iron ore, coal and lime are stored on the discharging quay. Iron ore is prepared in the sinter plant. Here, it is pounded, calibrated and cooked. Agglomerated iron ore and coke (produced from the coal in the coke plant), are blended by alternating the layers in the blast furnaces. Coke burning, by insufflation of hot air (1200°C), induced the fusion of the agglomerated iron ore that produced cast iron (94% of iron). Blast furnace slags are also recuperated and stocked. Cast iron is forwarded to the in-ladle metallurgy treatment installation where it is converting in steel. Cast iron is poured on scrap iron and the rest of carbon and impurity were eliminated using oxygen and argon. Steel obtained is put to the good content by introduction of metals as Al, Ti, Mn, Si, Cr, La, Ce or Ni for example. To finish, steel is solidified and molded.

15
16
17
18
19
20

**Table A.1:** Campaign's information for each complex.

22

Sampling time	Source	Site	Winds direction	Couple of samples collected
05/31/2013 06/03/13	**Complex 1** **Cast iron converter complex** (43°26'46.63''N / 4°53'51.50''E)	Upwind: **S3** (43°27'28.38''N / 4°53'36.58''E) Downwind: **S2** (43°25'35.97''N / 4°54'11.47''E)	**339° - 0°** (North winds)	7
10/29/2013 12/06/2013	**Complex 2** **Ore iron converter complex** (43°25'50.90''N / 4°52'51.45''E)	Upwind: **S5** (43°26'16.77''N / 4°52'40.20''E) Downwind: **S1** (43°25'15.17''N / 4°53'38.68''E)	**303° - 352°** (North winds)	8
07/04/2013 09/19/2013	**Complex 3** **Blast furnace slag storage area** (43°27'03.24''N / 4°52'56.50''E)	Upwind: **S3** (43°27'28.38''N / 4°53'36.58''E) Downwind: **S4** (43°26'34.87''N / 4°53'11.81''E)	**339° - 0°** (North winds)	4
12/14/13 01/24/14	**Ore terminal** (43°24'51.11''N / 4°52'21.66''E)	Upwind: **S6** (43°25'10.60''N / 4°52'2.54''E) Downwind: **S7** (43°24'49.58''N / 4°52'24.18''E)	**310° - 350°** (North winds)	9

23
24
25
26
27
28
29
30
31
32
33
34
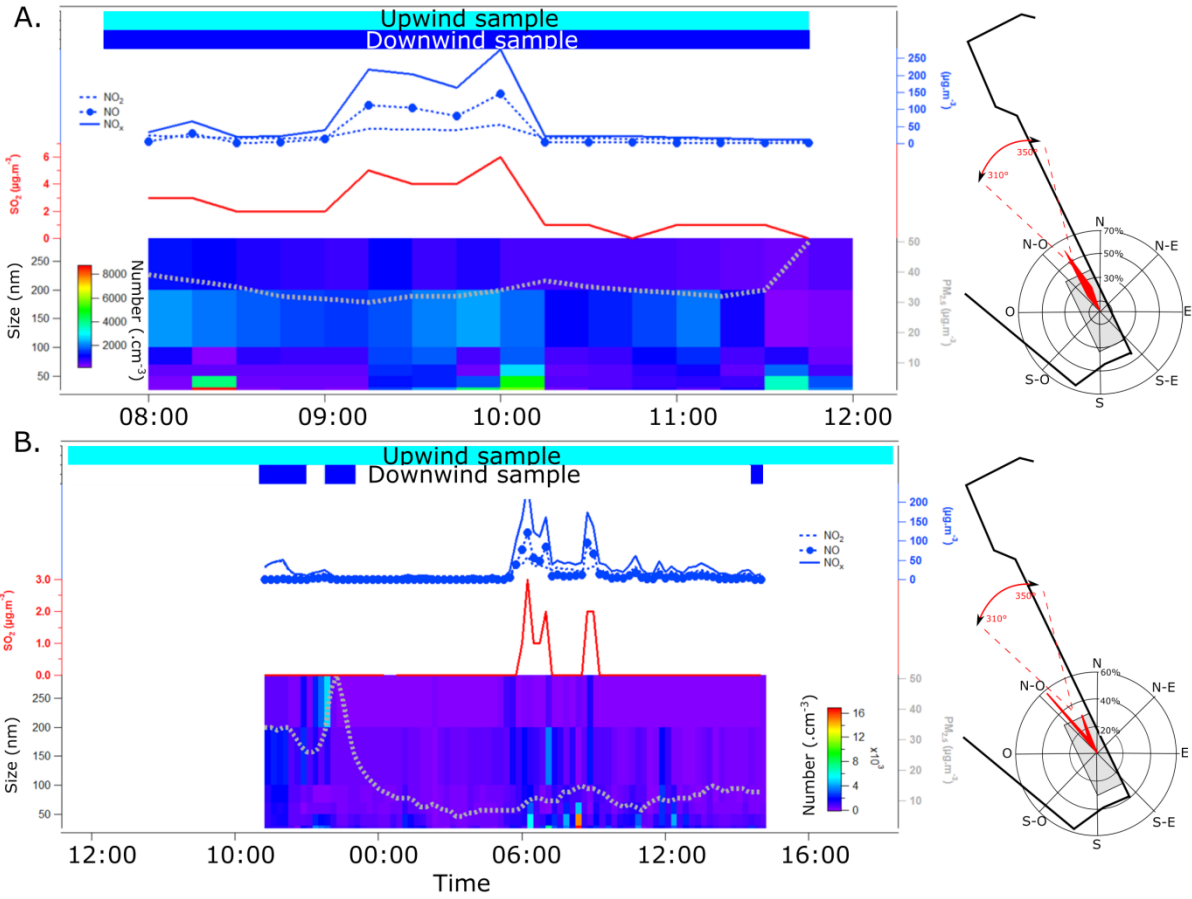
Figure A.1: **A.** Example of pair of samples selected and analyzed: Downwind and upwind samples were collected simultaneous. Pics of concentration going up to 250µg.m^{-3} for NOx, 150µg.m^{-3} for NO, 50µg.m^{-3} for NO$_2$ and 7µg.m^{-3} for SO$_2$ were observed on the downwind site when samples were collected. A high and constant PM2.5 concentration (between 30 and 50µg.m^{-3}) was observed with some episode with fine particle (20-50nm, going up to 8000 particles.cm^{-3}). These couple of sample was selected. **B.** Example of pair of samples not selected for further analysis.